Available online at www.sciencedirect.com
SCIENCE DIRECT®

Journal of the European Ceramic Society 24 (2004) 3195–3201
www.elsevier.com/locate/jeurceramsoc

Dual behavior of $CaCO_3$ as a porosifier and sintering aid in the manufacture of alumina membrane/catalyst supports

Cavus Falamaki*, Mehdy Naimi, Alireza Aghaie

Materials and Energy Research Center, PO Box 14155-4777, Tehran, Iran

Received 21 April 2003; received in revised form 11 October 2003; accepted 25 October 2003

Abstract

High permeability alumina membrane/catalyst supports have been prepared using $CaCO_3$ as inorganic porosifier. Green compacts had been formed by uniaxial compaction. The effect of porosifier initial content (1–7 wt.%) and sintering temperature (1325–1400 °C) on the permeability and porous structure (average permeable pore diameter and tortuosity) of the final products have been investigated. For any porosifier initial content in the range of 1–7 wt.%, there exists an optimum sintering temperature of 1350 °C corresponding to the highest permeability. Maximum permeability is obtained using 5 wt.% initial porosifier content. It is demonstrated that such enhanced permeabilities are not due to a pore growth mechanism. Instead, they are a result of tortuosity decrease due to a ''round pore shaping'' mechanism induced by the establishment of a liquid-phase sintering process.

Keywords: Al_2O_3; $CaCO_3$; Membranes; Microstructure-final; Sintering; Tortuosity

1. Introduction

Ceramic catalyst and membrane supports manufactured by controlled sintering of green compacts need to have a uniform degree of porosity. This may be achieved using organic or inorganic burnout materials. Organic porosifiers usually leave leachable residues affecting adversely the performance of catalysts supported on carriers.[1] On the other hand, the burnout process may pose sever environmental problems. Inorganic porosifiers may be used, as long as the catalytic performance of the final catalyst is not impaired. Alumina catalyst supports used in steam reforming may contain up to 10 wt.% alkaline earth metal oxides like calcium.[1] As a ceramic membrane support for liquid micro and ultrafiltration, such a content of metal oxide is tolerable for most applications. If calcium carbonate is chosen as the source of calcium, a dual behavior in the manufacturing process may be expected: porosifier and sintering aid. Both properties are desired, although the latter may reduce porosity after a certain firing stage. Therefore, the processing parameters for the use of $CaCO_3$ as a porosifier and sintering aid should be optimized. The open literature contains few such investigations.

The support surface roughness is a determining factor in the production of multilayer micro and mesoporous ceramic membranes. Usually large pores and high roughnesses are chosen for the first support layer despite the fact that there is then need for additional intermediate layers.[2] This is due to the high permeability. Using smaller pore sizes (i.e. using finer initial powders) is accompanied by a lower surface roughness. Nonetheless the latter may be applied only if the permeability could be enhanced using special techniques. In the case of membranes produced from fine alumina powders, this can be achieved by implementing several methods: conduction of the sintering process through a ''pore growth'' regime,[3] introduction of homogeneous macropores via the RBAO route through the liquid-gas reaction regime[4] and use of porosifiers ($CaCO_3$ in the present study).

* Corresponding author. Fax: +98-0262-62-21-888.
E-mail address: c-falamaki@merc.ac.ir (C. Falamaki).

0955-2219/$ - see front matter © 2003 Published by Elsevier Ltd.
doi:10.1016/j.jeurceramsoc.2003.10.041

2. Experimental

An alumina powder (Martinswerke, KMS-96) with the following typical analysis was used: Al_2O_3 96.00, Na_2O 0.20, K_2O 0.05, SiO_2 3.00 and MgO 0.10 wt.%. The average granule size of the latter was 160 μm. An Iranian calcium carbonate (0.17 wt.% SiO_2, 0.11 wt.% P_2O_5 and 0.062 wt.% Fe_2O_3 the main impurities) and PVA (4 cm^3 of a 2 wt.% aqueous solution per 100 g dry powder $CaCO_3+Al_2O_3$) were added to the alumina powder and the mixture was gently manually blended for 24 h. The resulting powder was fast milled for 10 min using zirconia balls. Some 1 g of the final powder was used to form disk shaped green compacts (diameter = 20 mm) by applying a uniaxial compression pressure of 61.8 MPa. The green compacts were heated up to the sintering temperature (1325, 1350, 1375 and 1400 °C) with a heating rate of 3 °C min^{-1}. The soaking time was 1 h.

Phase and microstructure analysis of the obtained samples were performed by X-ray diffraction (Siemens D500 diffractometer) and SEM (Stereo Scan 360-Leica, Cambridge). Density and porosity were measured according to ASTM C 373-88. Wet and dry permeability tests were done according to ASTM F 316 using a special holder made in our laboratory.[5] Simultaneous thermogravimetric-differential thermal analysis (STA) was carried out using a Polymer Laboratories apparatus using a heating rate of 5 °C min^{-1}. Specific surface area analysis was done using a Micromeritics apparatus. Four point flexural strength measurements were performed on 58.0×14.5×3.8 mm^3 rectangular bars with a mechanical testing machine (Instron model 1196). Surface roughness was measured using a TR100 surface roughness tester (TIME).

3. Results and discussion

The STA diagram for a sample initially containing 7 wt.% $CaCO_3$ is shown in Fig. 1. The first endothermic peak relates to the decomposition of $CaCO_3$ in the temperature range 450–680 °C. The CaO thus obtained is an activated oxide, apt to react with the alumina main core. The endotherm observed at 1320.6 °C may be attributed to such a reaction. The XRD diagrams of sintered (1375 °C) initial compacts containing 1, 3 and 7 wt.% $CaCO_3$ are shown in Fig. 2. Along with the initially present α-alumina phase, distinct peaks of $Ca_2Al_2SiO_7$ could be identified. The pertaining JCPDS card number is 35-755. It is observed that the peaks area of the $Ca_2Al_2SiO_7$ phase increases significantly with increasing initial concentration of $CaCO_3$ in the green compact. A few additional unidentified very weak peaks present were attributed to other calcium aluminates formed. The calcium aluminates peaks did not show any significant change with the variation of initial $CaCO_3$ content. This can be explained as follows.

During the thermal treatment, three main reactions occur:

$$CaCO_3 = CaO + CO_2, \qquad T < 800\,^{\circ}C \tag{1}$$

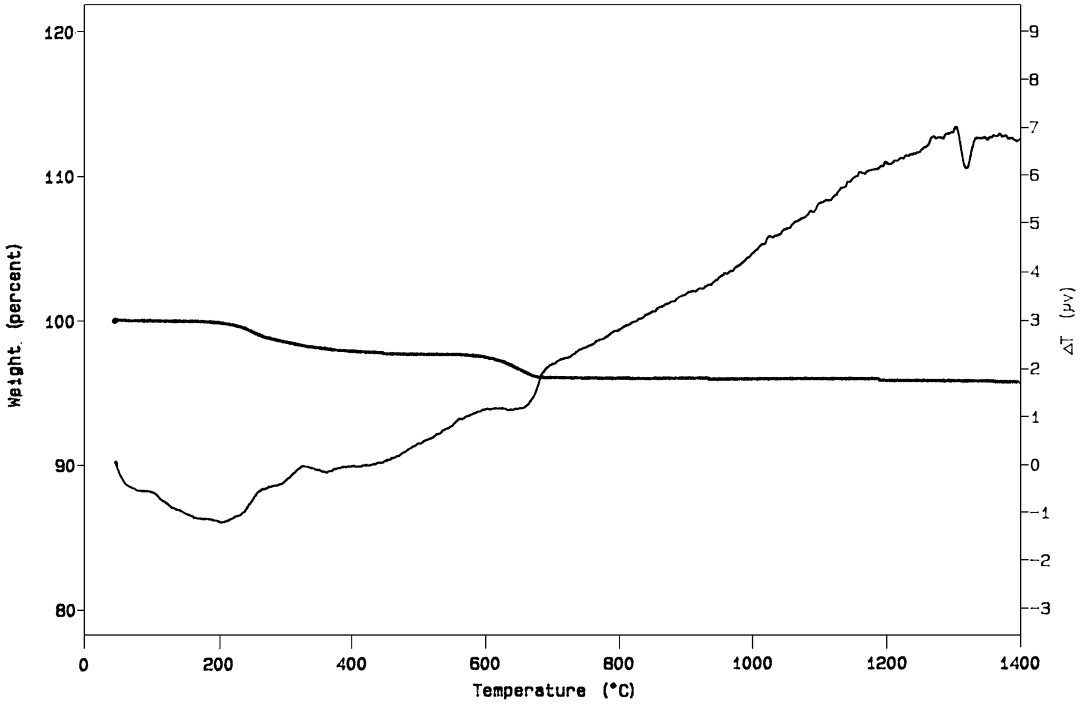

Fig. 1. STA diagram of a section of a green compact initially containing 7 wt.% $CaCO_3$.

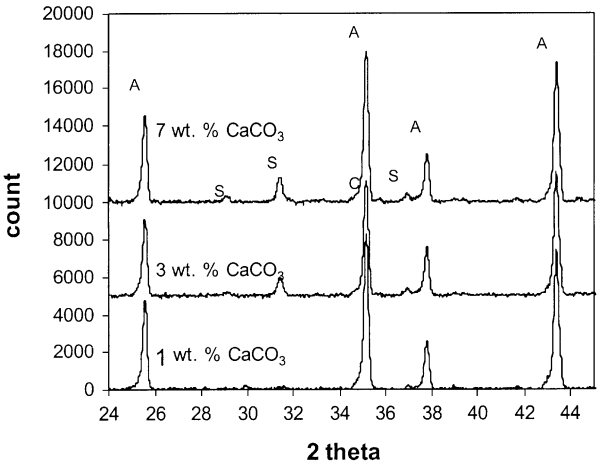

Fig. 2. XRD patterns for samples containing initially 1, 3 and 7 wt.% $CaCO_3$ (A = alumina, S = $Ca_2Al_2SiO_7$, C = C_mA_n phase).

$$mCaO + nAl_2O_3 = Ca_m(Al_2O_3)_n, \quad T > 1200\,^{\circ}C, \quad m \geqslant 1, \quad n \geqslant 1 \tag{2}$$

$$2CaO + SiO_2 + Al_2O_3 = Ca_2Al_2SiO_7, \quad T > 1200\,^{\circ}C \tag{3}$$

Reactions (2) and (3) compete with each other, reaction (3) being faster. At 7 wt.% initial $CaCO_3$ concentration, the SiO_2 content of the green compact is still higher than the stoichiometric amount needed to consume all the available CaO produced through reaction (1).

The open porosity dependence on temperature and initial $CaCO_3$ concentration is shown in Fig. 3. For each initial concentration of $CaCO_3$, the porosity decreases with increase in the sintering temperature (trivial). It is observed that this behavior is more pronounced for sintering temperatures higher than 1350 °C. For each constant sintering temperature, increasing the initial porosifier content has the result that the porosity approaches a maximum and then decreases. The initial increase is mainly attributed to the void production due to $CaCO_3$ decomposition. On the other hand, CaO acts as a sintering aid for alumina. These opposite functions result in a maximum in the porosity versus initial $CaCO_3$ concentration. The latter behavior is more pronounced for temperatures higher than 1350 °C, eventually due to more pronounced sintering.

The permeability curves are shown in Fig. 4. The data belong to the Knudsen flow regime where the flow rate through the specimens was independent of pressure. For each sintering temperature, permeability increases with the increase of $CaCO_3$ initial content up to 5 wt.% and then decreases. On the other hand, the permeabilities of specimens sintered at 1350 °C are larger than the corresponding values for the other temperatures. Considering the membrane support application, high permeabilities are desired.

The determination of the porous structure of the specimens has been performed using the single gas permeation data. A good agreement between mean pore radius determination by the nitrogen gas permeation method and mercury porosimetry has been already reported for alumina membranes.[6] The flow of nitrogen (which can be reasonably considered a non-condensable, non-adsorbable gas at RT) through a porous media can be divided into three main regimes depending on the Knudsen number: pure Knudsen (I), transition (II) and pure viscous flow (III). A typical permeation versus pressure diagram is shown in Fig. 5. It is observed that the pressure range employed covers all the three regimes aforesaid. The permeability in the Knudsen regime is constant (independent of pressure) and may be related to the porous structure characteristics through the following relation:

$$F_k = \frac{2\varepsilon r_{avg}}{3\tau}\left(\frac{8}{\pi RTM}\right)^{0.5} \tag{4}$$

where F_k is the permeability (mol s^{-1} m^{-2} Pa^{-1}), r_{avg} the average pore diameter (m), ε the porosity, τ the tortuosity, R the universal gas constant (J mol^{-1} K^{-1}), T the temperature (K) and M the gas molecular mass (kg kg mol^{-1}).

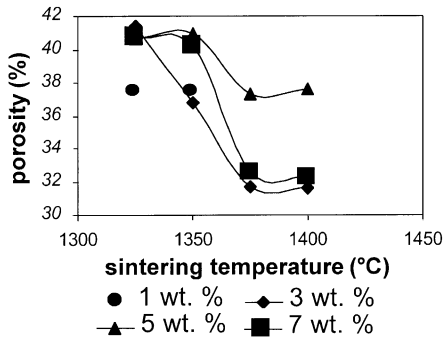

Fig. 3. Dependence of open porosity on sintering temperature and initial $CaCO_3$ content.

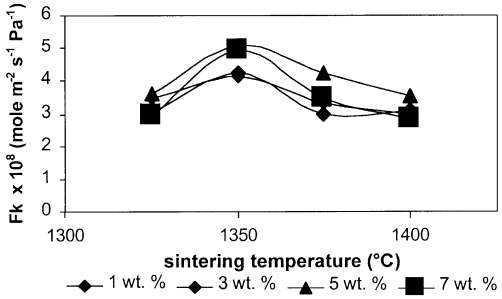

Fig. 4. Permeability as a function of sintering temperature and initial $CaCO_3$ content.

At high pressures, the curve transforms into a straight line, which, by extrapolation passes through the origin. The latter section is a pure viscous flow regime whose slope may be correlated as below:

$$S = \frac{\varepsilon r_{\text{avg}}^2}{8\eta\tau RTL} \tag{5}$$

where S is the slope (mol s^{-1} m^{-2} Pa^{-2}), L the membrane thickness (m) and η is the gas viscosity (kg m^{-1} s^{-1}). Table 1 summarizes the experimental values of S. Using Eqs. (4) and (5) and based on the permeation data, r_{avg} and τ have been evaluated for the specimens sintered at 1325, 1350 and 1400 °C. The results are shown in Figs. 6–8. It is observed that for each sintering temperature and increasing the initial porosifier content, the average pore diameter increases to a maximum and then decreases. In all cases, the maximum average pore diameter corresponds to the $CaCO_3$ initial content of 5 wt.%. The trend is very similar to that of the porosity changes with initial porosifier content. The same explanation also holds. Instead, the curious fact is that for all the $CaCO_3$ initial contents, the average pore diameter for the sintering temperature 1350 °C lies between 1325 and 1400 °C. That is, the higher permeabilities for all the samples sintered at 1350 °C may not be correlated to a "pore growth" phenomenon. The use of the pore growth mechanism within the initial stage of sintering for the manufacture of alumina membrane supports has been recently reported and treated in detail by Falamaki et al.[3] They used the same alumina powder but applying a compaction pressure of 31.2 MPa. A maximum in the permeability versus pressure curve was observed at a certain sintering temperature which was mainly attributed to pore growth (and to a lesser extent to tortuosity decrease) during the initial stage of sintering. Such a maximum has been also observed in the present study for samples containing no initial $CaCO_3$ (permeabilities equal to 3.49, 4.06 and 3.44×10^{-8} mol m^{-2} s^{-1} Pa^{-1} for samples sintered at 1350, 1375 and 1400 °C, respectively). As described in the work of Falamaki et al.,[3] the pore growth phenomenon is accompanied by a sharp decrease in surface area due to the elimination of small (high specific area) entities. The prevailing mechanisms involved have been discussed by Zheng and Reed.[7] The BET multipoint surface area of the samples with an initial porosifier content of 5 wt.% are shown in Fig. 9. No such abrupt decrease is observable. As it will be explained, introduction of $CaCO_3$ changes completely the alumina microstructure evolution trend with increasing sintering temperature.

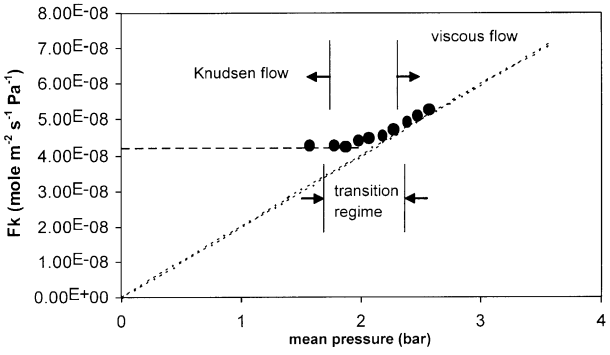

Fig. 5. A typical permeability versus mean pressure curve showing three distinct flow regimes (sintering temperature 1350 °C, initial $CaCO_3$ content 1 wt.%).

Table 1
Values of $S\times10^{12}$ (mol m^{-2} s^{-1} Pa^{-2}) used in Eq. 5

Sintering temperature (°C)	$CaCO_3$ wt.%	$CaCO_3$ wt.%	$CaCO_3$ wt.%	$CaCO_3$ wt.%
	1	3	5	7
1325	6.32	6.28	8.80	8.11
1350	6.41	7.38	11.85	9.65
1400	4.05	4.05	8.11	4.05

According to Fig. 7, considering an initial $CaCO_3$ content of 5 wt.%, the tortuosity decreases from 5.76 (sintering temperature 1400 °C) down to 1.95 (sintering temperature 1350 °C). The approximate 300% reduction in tortuosity is accompanied with only a 7% pore size enlargement. On the other hand, the porosity is about 0.375 for both samples. Therefore it may be concluded that higher permeabilities observed at 1350 °C are merely due to a less tortuous path along the pores. Considering the sintering temperatures 1325 and 1400 °C, it is observed that tortuosity attains a rather distinct maximum at 5 wt.% initial porosifier content.

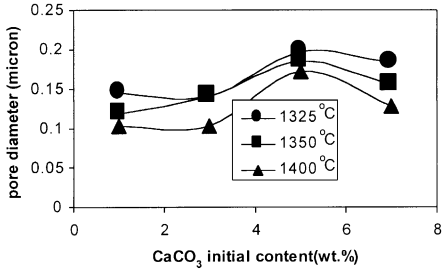

Fig. 6. Average permeable pore diameter as a function of sintering temperature and initial $CaCO_3$ content.

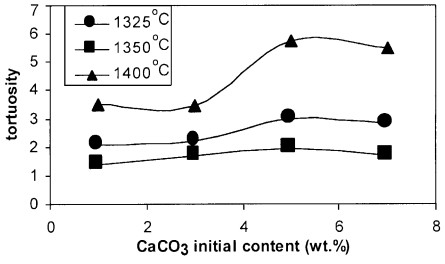

Fig. 7. Tortuositiy as a function of sintering temperature and initial $CaCO_3$ content.

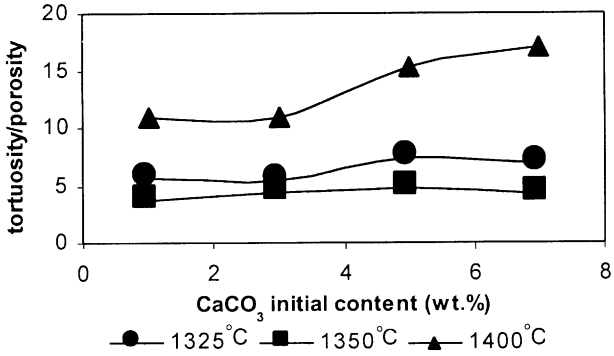

Fig. 8. Ratio of tortuosity over porosity as a function of sintering temperature and initial $CaCO_3$ content.

This is less pronounced for the 1350 °C sintering temperature. The ratio of tortuosity over porosity as a function of porosifier content and sintering temperature for different samples has been shown in Fig. 8. The latter follows the same trend as tortuosity as observed in Fig. 7. Therefore, according to Figs. 7 and 8, the higher permeabilities observed for the 1350 °C sintering temperature in Fig. 4 are surprisingly due to a strong decrease in tortuosity.

Actually, the largest pores (at each initial $CaCO_3$ content) are just produced during the decomposition of the porosifier (<1000 °C). In the temperature range of 1325–1400 °C, pore size reduction occurs as a result of enhanced shrinkage eventually due to a liquid phase sintering mechanism. The production of low melting calcium–aluminate [like as reaction (2)] and calcium–aluminate–silicate species is responsible for such a

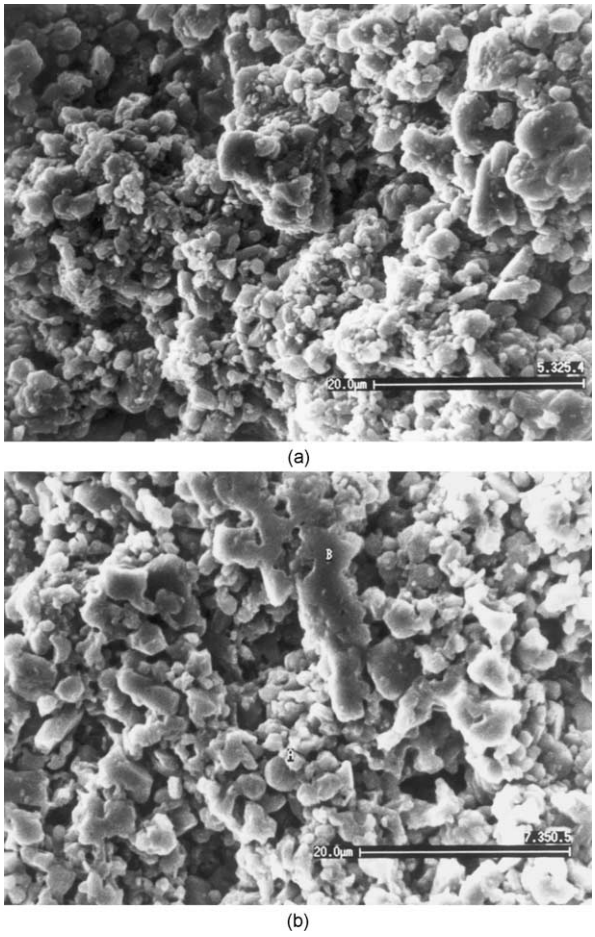

Fig. 10. SEM pictures of samples (a) initially containing 5 wt.% $CaCO_3$ sintered at 1325 °C and (b) initially containing 7 wt.% $CaCO_3$ sintered at 1350 °C.

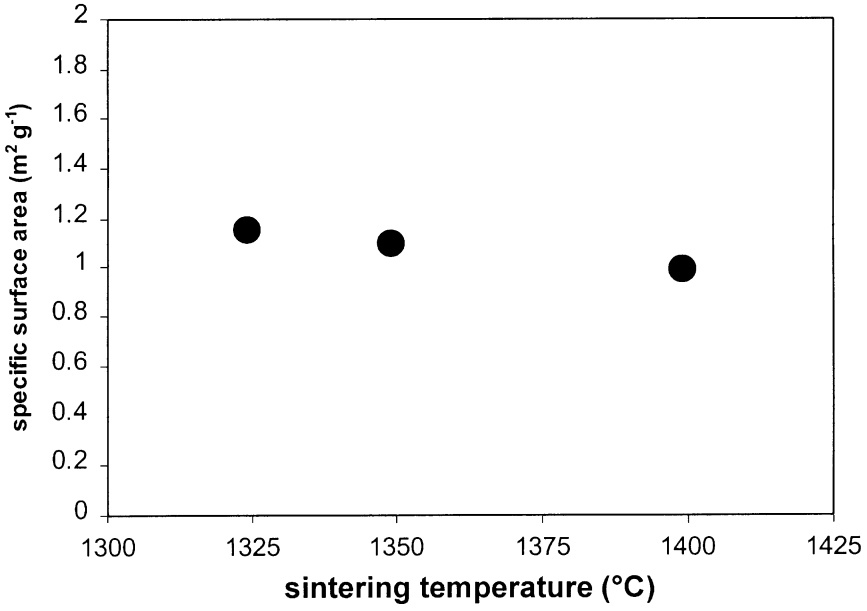

Fig. 9. BET multipoint surface area of samples with an initial porosifier content of 5 wt.%.

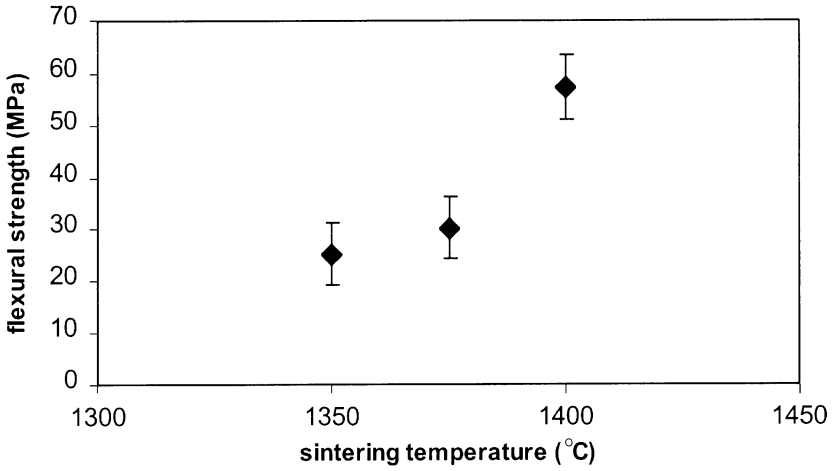

Fig. 11. Flexural strength as a function of sintering temperature for a 5 wt.% initial $CaCO_3$ content.

mechanism. This process is more pronounced for lower (= <3 wt.%) initial porosifier content. Higher contents produce initially larger pores, which shrink with a much slower rate. For the latter case and in the temperature range 1325–1350 °C, sintering is mainly accompanied with changes in pore shape (more round pores). Tortuosity used in Eq. 4 refers to many effects influencing gas transport: path length, interconnectivity, roughness, etc.[8] Hence, it may be deduced that the decrease in tortuosity between 1325 and 1350 °C is mainly due to a reduction in roughness due to a more round pore shape.

Micrographs of two samples containing 5 and 7 wt.% initial porosifier content and sintered at 1325 and 1350 °C, respectively, are shown on Fig. 10 (a,b). These samples are approximately of the same porosity (ca. 0.4). The measured mean diameter of the latter sample is about 20% smaller, while the permeability is around 30% larger. The authors of this work attribute this fact to the more "roundness" of the particles and hence, less roughness of the pores.

Roughness measurements performed on different samples showed no significant dependence on initial $CaCO_3$ content or sintering temperature. All surface roughnesses (R_a) lie in the range of 0.6–0.8 μm. Wet permeation experiments showed that the largest active pores (corresponding to the bubble point) were in the size range of 0.61–0.74 μm. The latter are considered mainly as powder inhomogeneity effects during the compaction stage and not to internal microcracks formed during the firing stage.

Concerning the permeance characteristics, the sample containing initially 5 wt.% $CaCO_3$ content and sintered at 1350 °C is the optimum one. Fig. 11 shows the flexural strength for the samples sintered at 1350, 1375 and 1400 °C containing initially 5 wt.% porosifier. Although the mechanical strength of the optimum sample is the lowest, but its absolute value is quite reasonable, being approximately 25 MPa.

4. Conclusions

High permeability alumina membrane/catalyst supports have been prepared using $CaCO_3$ as inorganic porosifier. It is shown that, for any porosifier initial content in the range of 1–7 wt.%, there exists an optimum sintering temperature of 1350 °C corresponding to the highest permeability. Maximum permeability is obtained using a 5 wt.% initial porosifier content. It is demonstrated that such a maximum is not due to a pore growth mechanism. Instead, it is a result of tortuosity decrease due to a "round pore shaping" mechanism induced by the establishment of a liquid-phase sintering process.

During the firing process, porosity initially increases due to the release of CO_2 gas. During the soaking time, two main processes take place: Tortuosity decrease due to a "pore shape rounding" effect and simultaneous pore size decrease and tortuosity increase due to shrinkage. The former is accompanied by insignificant changes in total porosity. A minimal addition of $CaCO_3$ (1 wt.%) eliminates any pore growth mechanism due to the establishment of a liquid-phase sintering process. By properly choosing process parameters such as sintering temperature and porosifier initial content, it is possible to make the "round pore shaping" mechanism dominate and hence to obtain an enhanced permeability.

References

1. Gerdes, H. W., Remus, D. J. and Szymansky, T., Method of making porous catalyst carrier without the addition of forming agents. US Patent 5 733 842, 1998.
2. Bonekamp, B. C., Preparation of asymmetric ceramic membrane supports by dip-coating. In *Fundamentals of Inorganic Membrane Science and Technology*, ed. A. J. Burggraaf and L. Cot. Elsevier Science, Netherlands, 1996, pp. 140–225.

3. Falamaki, C., Shafaie Afarani, M. and Aghaie, A., Initial stage pore growth mechanism applied to the manufacture of ceramic membrane/catalyst supports. *J. Eur. Cer. Soc.* (in press).
4. Falamaki, C., Aghaie, A. and Ardestani, N. R., RBAO membranes/catalyst supports with enhanced permeability. *J. Eur. Cer. Soc.*, 2001, **21**, 2267–2274.
5. Falamaki, C., Aghaie, A. and Ardestani, N. R., Iranian Patent 26 446, 2000.
6. Uchityl, P., Gas permeation in ceramic membranes: Part I. Theory and testing of ceramic membranes. *J. Membrane Sci.*, 1994, **97**, 139–144.
7. Zheng, J. and Reed, J. S., The different roles of forming and sintering on densification of powder compacts. *Am. Cer. Soc. Bull*, 1992, **71**(9), 1410–1416.
8. Burggraaf, A. J., Transport and separation properties of membranes with gases and vapours. In *Fundamentals of Inorganic Membranes, Science and Technology*, ed. A. J. Burggraaf. Elsevier, Netherlands, 1996, pp. 341.